C-BAND SEA ICE MODEL

Jeroen Verspeek, Ad Stoffelen, Siebren de Haan
KNMI, Postbus 201, 3730 AE de Bilt, the Netherlands
Jeroen.Verspeek@KNMI.nl

ABSTRACT

Using the scatterometer data from the ERS-2 satellite, a classification algorithm for sea/ice discrimination, based on Bayesian statistics is introduced. Also a comparison with ice maps obtained by other models and measurements is made.

The differences in backscatter properties between water and ice can be used to infer discrimination criteria. Ice has isotropic backscatter properties. Water on the other hand has anisotropic backscatter properties, which fact is used to retrieve wind direction. Traditionally people have used simple parameters representing the geophysical properties of ice, like an anisotropy coefficient. Another approach is to use a geophysical model function (GMF) that describes the measurement backscatter data as a function of one or more physical parameters. This method is used for wind retrieval but can be equally well applied for ice retrieval. It has the advantage that the full information content of the measurements is used.

For wind the backscatter GMF naturally is dominated by two parameters, being the wind speed and wind direction. For ice, plots of measured triplets in σ^0 -space show that in good approximation all ice points lie on a straight line. This means that the ice GMF can be described with one geophysical parameter named a, being the abscissa along this line. The sea ice GMF is constrained to fit the measurement space sea line for all across-swath wind vector cells. A quasi-linear incidence angle (θ) dependency results. Retrieval of the ice parameter a is carried out by projecting the measured backscatter triplet onto the ice line. The in the sea ice community commonly-used σ^0 (θ= 40°) is then equal to GMF(a, θ= 40°).

Based on the distance of a measured σ^0 -triplet to the ice line and to the wind cone, a Bayesian algorithm can classify the point as ice or as water.

1. INTRODUCTION

ERS scatterometer winds have proven to be very useful for the analysis and forecasting of dynamic weather [1]. Increased coverage, such as from tandem ERS-1 and ERS-2 measurements [2], clearly improves the usefulness in extreme events. After the development of improved data characterisation and assimilation procedures, operational use of SeaWinds and ERS-2 at among others KNMI [3], ECMWF [4] and CNMCA [10] for Numerical Weather Prediction (NWP) is a fact, while shift meteorologists are using the ERS-2 data for nowcasting. Moreover, wind conditions drive the ocean circulation that in turn plays a major role in the climate system and in ocean life (e.g., fisheries).

Both scatterometer research and development, and routine processing and monitoring are funded by EUMETSAT through the Satellite Application Facilities (SAFs). More specifically, the Royal Netherlands Meteorological Institute (KNMI) participates in the Ocean and Sea Ice (OSI) SAF [5], the Climate Monitoring (CM) SAF, and the NWP SAF for these purposes. In the context of these SAFs KNMI provides software and data with:

- Tailor-made scatterometer quality control (QC) in order to avoid unrepresentative wind data (e.g. rain contaminated or sea state, see, *Portabella and Stoffelen*, 2002);
- Sea ice screening;
- Generic scatterometer backscatter data inversion;
- Procedure to average backscatter measurements in a resolution cell of varying size, in order to provide spatially representative and accurate winds for NWP models;
- Generic scatterometer cost function to cope with all kinds of scatterometer data;
- Routine processing and monitoring of wind and, in the near future, surface stress;
- Web-based product presentation, and distribution by FTP;
- Scatterometer processing software;
- Web-based monitoring reports.SAF activity is currently mainly focused on SeaWinds, although much of the algorithms are generically applicable for the ERS scatterometer and ASCAT on METOP, to be launched in 2005. KNMI is seeking user participation in a Visiting Scientist programme or as beta user, aiding in the development of our software or data products.

One of the SAF activities is in scatterometer sea ice screening. To this end a sea ice model has been developed.

2. C-BAND SEA ICE MODEL

Figure 1 schematically depicts the distribution of ERS backscatter triplets in 3D measurement space [7]. This is the space spanned by plotting all triplets of ($\tilde{\sigma}_{fore}$, $\tilde{\sigma}_{aft}$, $\tilde{\sigma}_{mid}$) along the (x, y, z) axes respectively. Sea ice points lie close to an ice line denoting a linear variation in the backscatter triplet with varying ice condition, whereas wind points are close to a conical surface along which prime axis the wind speed varies, and along its circumference the wind direction varies.

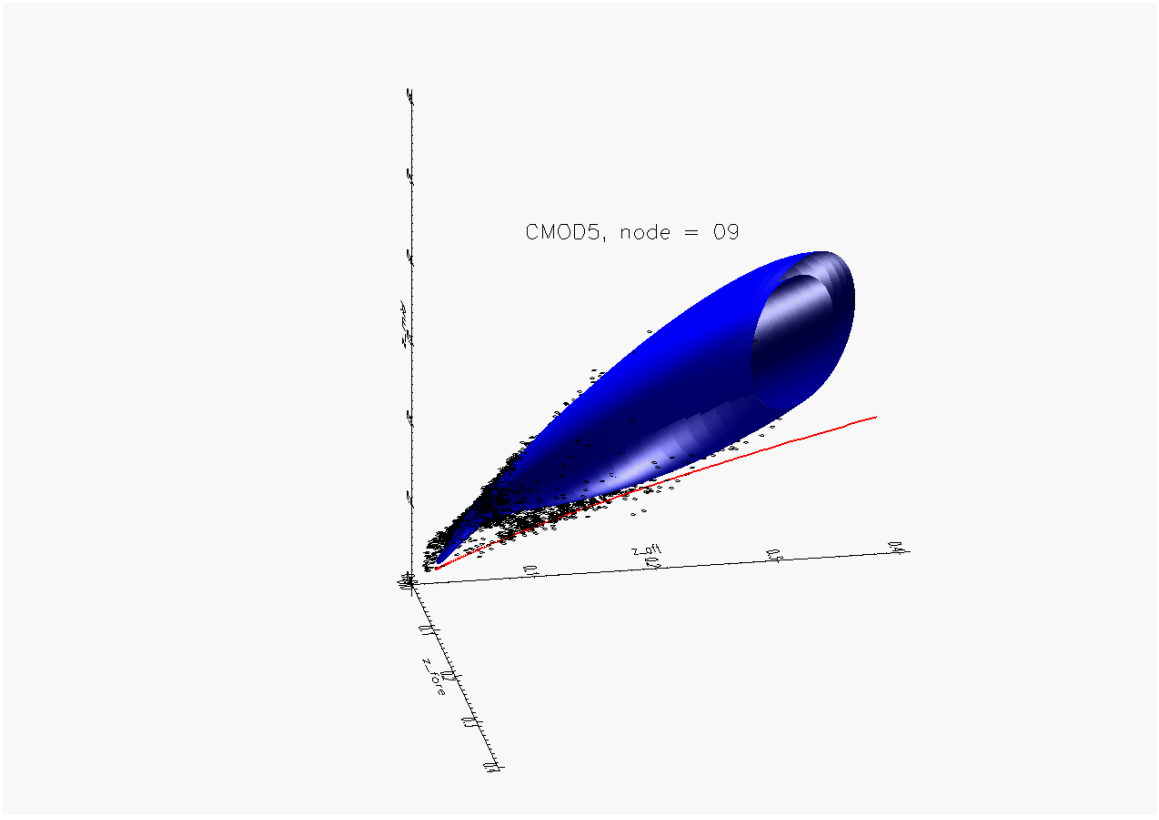

Figure 1. ERS scatterometer measurement space for Wind Vector Cell or node 9. The thick red line represents the ice line, whereas the curved conical shape represents the windcone. The black dots are measured σ^0 triplets.

Figure 2. Segregation of ice (red) and water (blue) points using an approximate sea ice map. Top left is for triplets with fore backscatter within 0.2 dB of aft backscatter versus mid beam backscatter for a inner swath WVC. Top right plot is made for mean fore plus aft backscatter of –15 dB (red vertical line in left plot) with again 0.2 dB margin. Bottom plots shows for WVC 1 fore versus aft backscatter (left) and fore backscatter within 0.2 dB of aft backscatter versus mid beam backscatter. Ice line (dotted) and wind cone (solid lines) are also shown. It is clear that the sea ice mask contains wind cone points and mixed sea ice/water points.

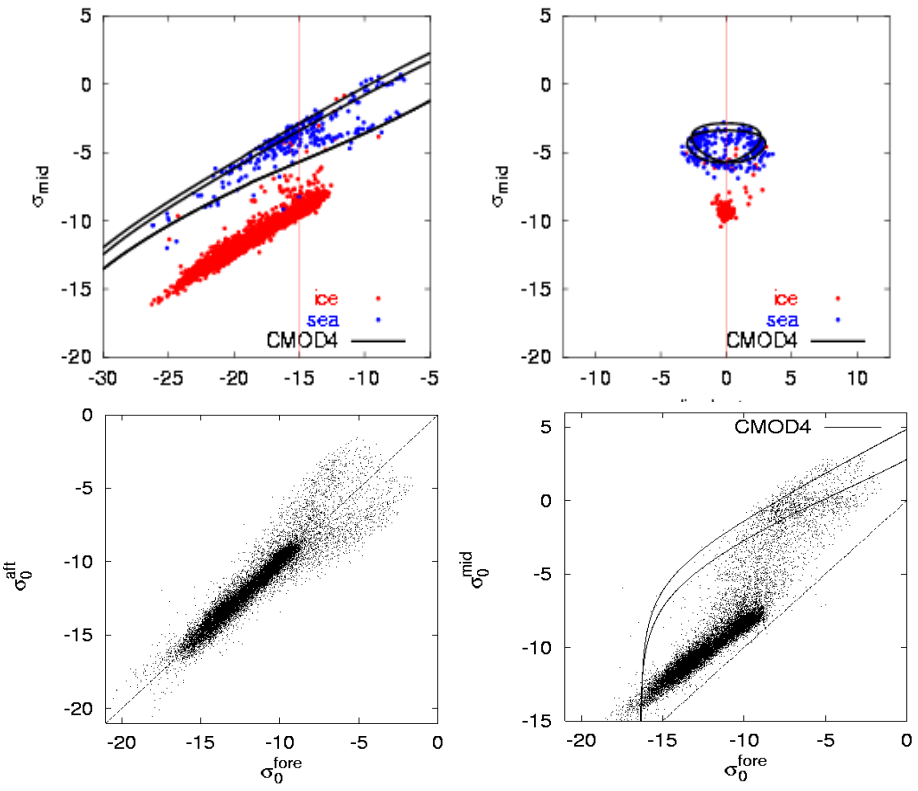

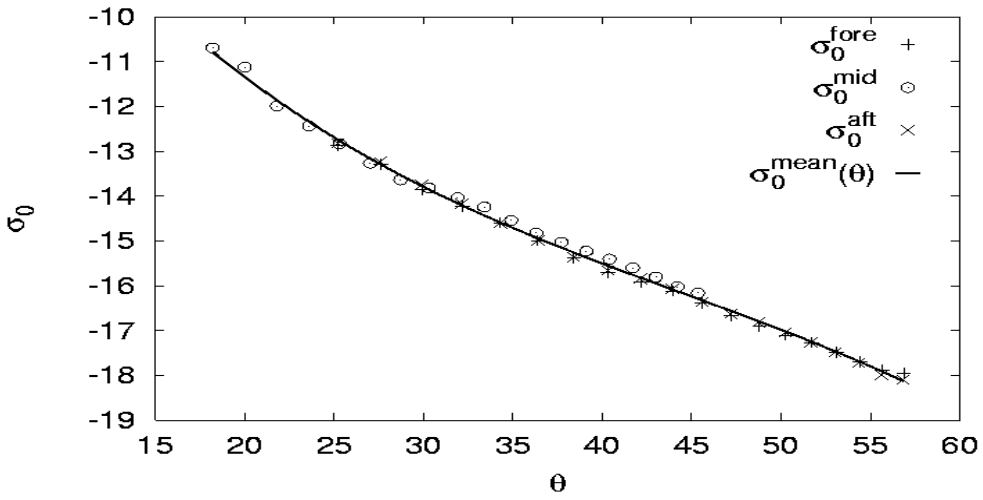

Figure 3. Sea ice GMF mean backscatter (solid line) versus individual fore, mid, and aft backscatter values. The mean backscatter at a particular incidence angle is rather consistent over sea ice surface between the three beam measurements.

Figure 3 shows the consistency of fore, mid and aft beam measurements as a function of radar beam incidence angle. Residual differences are small and at the level of instrument calibration [8]. As such, it is planned to use the sea ice model presented here for calibration of the C-band ASCAT scatterometer on METOP, among other methods.

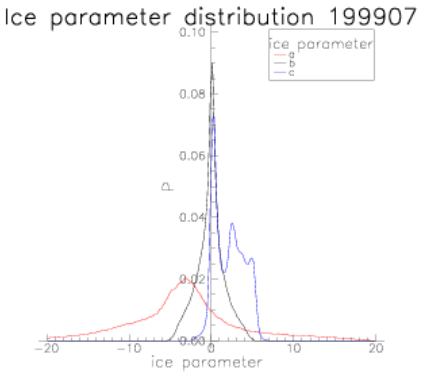

Figure 4. Distribution of the a, b, and c ice coordinates for a dataset containing wind and ice points. Clearly the wind-points can be distinguished as an addition to the distribution of the c-coordinate.

In the measurement space another coordinate system ($\mathbf{e_a}$, $\mathbf{e_b}$, $\mathbf{e_c}$) is defined relative to the ice line. Coordinate *a* is the abscissa along the ice line, *b* and *c* are the coordinates perpendicular to the ice line, where $\mathbf{e_c}$ is lying in the plane $\sigma_{fore} = \sigma_{aft}$. Parameter *a* is a geophysical parameter representing the ice age, parameters *b* and *c* define the distance of a measurement to the ice line. In constructing the ice model these ice parameters have been scaled to a normal distribution with average zero and standard deviation of 1 for a measurement set containing only ice points. Figure 4 shows the distribution of these parameters for a measurement set containing both wind- and ice points. The *b* and *c* parameters are centred around the vertical axis, as expected. Parameter *a* shows an offset which is caused by the ice backscattter properties of the measurements. Because these backscatter properties vary over time and space, variations in the *a*-distribution are to be expected.

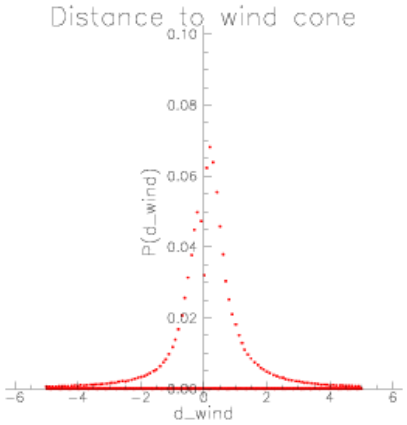

Figure 5. Distribution of the distance to the wind cone d_{wind} for a dataset containing wind and ice points.

Figure 5 shows the distribution of the distance to the wind cone for the same dataset that is used for figure 4. Also the distance to the wind cone is scaled so that the standard deviation is 1. A triplet measurement can be classified as either water or ice based on the distance to the wind cone and the distance to the ice line of that measurement in σ^0-space.

3. SEA ICE SCREENING

From Bayes probability theorem we derive

$$\frac{p(ice \mid \boldsymbol{\sigma}^0)}{p(water \mid \boldsymbol{\sigma}^0)} = \frac{p(\boldsymbol{\sigma}^0 \mid ice)}{p(\boldsymbol{\sigma}^0 \mid water)} \cdot \frac{p(ice)}{p(water)}$$

further noting that

$$p(ice \mid \boldsymbol{\sigma}^0) + p(water \mid \boldsymbol{\sigma}^0) = 1$$
$$p(ice) + p(water) = 1$$

this can be restated as

$$\text{logit}\,(p(ice \mid \boldsymbol{\sigma}^0)) = \ln\left(\frac{p(\boldsymbol{\sigma}^0 \mid ice)}{p(\boldsymbol{\sigma}^0 \mid water)}\right) + \text{logit}\,(p(ice))$$

where logit(p)=ln(p/(1-p). The a posteriori ice probability p(ice|σ0) is computed from the a priori ice probability p(ice) and the measurement probabilities, given either the ice or water condition, resp. p(σ0|ice) or p(σ0|water). These latter two are associated with the distances to the sea ice line and wind cone in measurement space respectively, and may thus be computed in deriving a geophysical product from the ERS scatterometer.

Note that the equation provides best discrimination for the many water points away from the sea ice line, or for the many ice points away from the wind cone. Remains that some ice and water points can coincide in the measurement space, thus providing no discrimination. In this case, the a priori knowledge is crucial. The a priori ice probability could be either simply based on a climatology, or on the recent history of ERS scatterometer passes. In our model the a priori probability is set to 0.5 to start with, and is combined with the swath measurement data from the ERS scatterometer on either an Arctic and Antarctic polar grid of 25 km, depending on the proximity of the poles. After computation of the a posteriori probability ratio and its associated ice screening, it is saved on the grid for subsequent passes.

To represent the probability of freeze and thaw processes, we slowly relax the a priori probability to the value of 0.5 (corresponding to zero for the logit). Since such freeze/thaw processes are more likely close to the ice edge, where the probability ratio gradient is high, we also test spatial relaxation. The spatial context (filter) represents the probability of change (freeze/thaw) given the proximity of the ice edge and the typical overpass cycle (12 hours). As such, p(ice)/p(water) is updated every pass, but temporally and spatially relaxed. Typical values used are 192 hour for the temporal, and 75 km for the spatial relaxation (1/e values). Outliers where both the distance to the ice line and to the wind cone is larger than three times the standard deviation are not taken into account. These points may be erratic measurement but it can also be that the footprint of the radar (50km x 50km) contains both areas of water and areas of ice. In such cases neither the wind cone nor the ice line can provide a good model for the measurement. For the middle part of the swath, the ice line lies close to the wind cone or intersects with it. In this case the discrimination between ice and water can be difficult, a measurement may lie close to both the ice line and the wind cone. By the use of spatial relaxation p(ice) will drift to 0.5 in such ice edge areas with outliers.

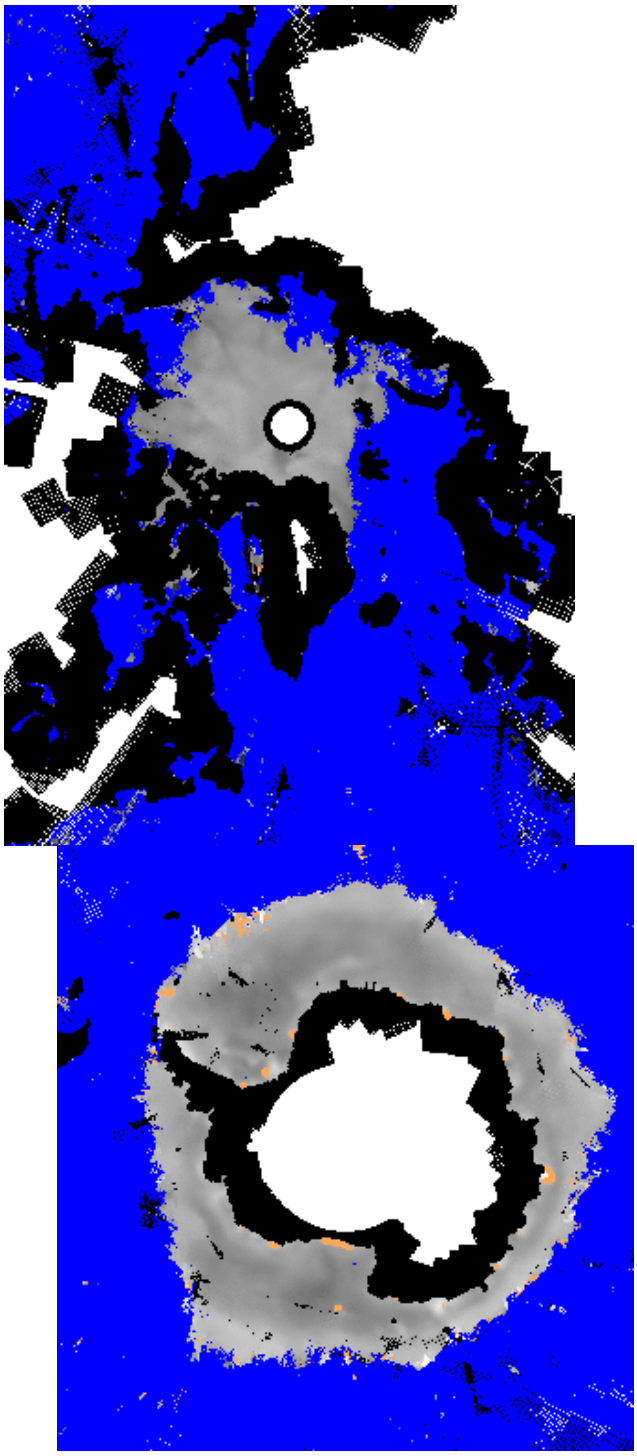

Figure 6. Map of the Arctic and Antarctic region of 1999/08/30. Blue indicates sea, grey represents the ice parameter a, and orange indicates areas where the standard deviation of the ice parameter is large.

Figure 6 shows a map of the Arctic and Antarctic region for subsequently overlaid orbits of ERS-2, made with the above described Baysian sea/ice discrimination algorithm. Blue indicates areas of water (p(water) > 0.5), black areas are covered by the satellite but without valid measurements, and the large white areas contain no products at all. The retrieved sea ice GMF parameter *a* is represented in the ice areas on a grey scale. White indicates a high value of *a* (high backscatter), and black a low value (low backscatter). Clearly a

structure in *a* is observed on the ice map. Orange areas are ice, but the standard deviation of *a* is larger that a certain value, thus the value of *a* cannot be determined with high reliability.

4. OUTLOOK

In 3D-measurement space a clear separation between wind and sea ice states is generally found. Moreover, combined ice/water states can be determined is some cases. By careful selection of sea ice points a consistent sea ice model is derived. The model is independent of season and geographical location and depends on one geophysical parameter, called *a*, and which is associated with ice age [8].

Besides the powerful wind probability measure from wind retrieval, ice probability is now being used for improved ice/water discrimination.

Moreover, consistent geophysical sea ice parameter maps can be made, which can also be used as prior information in sea ice screening. Moreover, areas with stable sea ice parameter can be useful for instrument calibration.

Hardware permitting, there will be a continuous series of C-band scatterometers with at times ideal coverage of the ocean surface wind in the coming two decades. EUMETSAT provides user services in collaboration with KNMI, where these are now being set up and freely available at http://www.knmi.nl/scatterometer [9] for the SeaWinds and ERS-2 scatterometers. Moreover, a visiting scientist scheme is funded in order to support the development programme and the use of the KNMI services. Near-real time FTP products or software can be obtained by sending a request to the author.

REFERENCES

1. Isaksen, Lars, and Ad Stoffelen, 2000, “ERS-Scatterometer Wind Data Impact on ECMWF’s Tropical Cyclone Forecasts”, IEEE-Transactions on Geoscience and Remote Sensing (special issue on Emerging Scatterometer Applications), Vol. **38** (4), pp. 1885-1892.

2. Stoffelen, Ad and Paul van Beukering, “The impact of improved scatterometer winds on HIRLAM analyses and forecasts”, BCRS study contract 1.1OP-04, report published by BCRS, Delft, The Netherlands, and HIRLAM technical report #31, published by IMET, Dublin, Ireland, 1997.

3. HiRLAM, 2002, High-Resolution Limited Area Model, http://hirlam.knmi.nl

4. ECMWF, 2002, European Centre for Medium-range Weather Forecast, http://www.ecmwf.int

5. Ocean & Sea Ice web site, 2005, http://www.osi-saf.org/index.php

6. Portabella, M., and Stoffelen, A., “A comparison of KNMI quality control and JPL rain flag for SeaWinds,” *Can. Jour. of Rem. Sens,* Vol. **28** (3), pp. 424-430,

7. Stoffelen, Ad, 1998, Scatterometry, thesis Un,. Utrecht, the Netherlands, http://www.library.uu.nl/digiarchief/dip/diss/01840669/inhoud.htm

8. Siebren de Haan and Ad Stoffelen, Ice Discrimination Using ERS scatterometer, http://www.knmi.nl/scatterometer/SCATandASCAT/pdf/SAFOSI_W_icescr-knmi.pdf

9. KNMI, 2005, http://www.knmi.nl/scatterometer